

The Role of Polymer Fractionation in Energetic Losses and Charge Carrier Lifetimes of Polymer: Fullerene Solar Cells

Derya Baran, Michelle S Vezie, Nicola Gasparini, Florent Deledalle, Jizhong Yao, Bob C. Schroeder, Hugo Bronstein, Tayebah Ameri, Thomas Kirchartz, Iain McCulloch, Jenny Nelson, and Christoph J Brabec

J. Phys. Chem. C, **Just Accepted Manuscript** • DOI: 10.1021/acs.jpcc.5b05709 • Publication Date (Web): 10 Aug 2015

Downloaded from <http://pubs.acs.org> on August 16, 2015

Just Accepted

“Just Accepted” manuscripts have been peer-reviewed and accepted for publication. They are posted online prior to technical editing, formatting for publication and author proofing. The American Chemical Society provides “Just Accepted” as a free service to the research community to expedite the dissemination of scientific material as soon as possible after acceptance. “Just Accepted” manuscripts appear in full in PDF format accompanied by an HTML abstract. “Just Accepted” manuscripts have been fully peer reviewed, but should not be considered the official version of record. They are accessible to all readers and citable by the Digital Object Identifier (DOI®). “Just Accepted” is an optional service offered to authors. Therefore, the “Just Accepted” Web site may not include all articles that will be published in the journal. After a manuscript is technically edited and formatted, it will be removed from the “Just Accepted” Web site and published as an ASAP article. Note that technical editing may introduce minor changes to the manuscript text and/or graphics which could affect content, and all legal disclaimers and ethical guidelines that apply to the journal pertain. ACS cannot be held responsible for errors or consequences arising from the use of information contained in these “Just Accepted” manuscripts.



The Role of Polymer Fractionation in Energetic Losses and Charge Carrier Lifetimes of Polymer: fullerene Solar Cells

Derya Baran^{1}, Michelle S. Vezie², Nicola Gasparini¹, Florent Deledalle², Jizhong Yao², Bob C. Schroeder³, Hugo Bronstein³, Tayebah Ameri¹, Thomas Kirchartz^{4,5}, Iain McCulloch³, Jenny Nelson², Christoph J. Brabec^{1,6}*

¹ Institute of Materials for Electronics and Energy Technology (i-MEET), Friedrich-Alexander University of Erlangen-Nuremberg, Martensstraße 7, 91058, Erlangen, Germany

² Center for Plastic Electronics, Department of Physics, Imperial College London, London SW7 2AZ, United Kingdom

³ Center for Plastic Electronics, Department of Chemistry, Imperial College London, London SW7 2AZ, United Kingdom

⁴ IEK5-Photovoltaics, Forschungszentrum Jülich, 52425 Jülich, Germany

⁵ Faculty of Engineering and CENIDE, University of Duisburg-Essen, Carl-Benz-Straße 199, 47057 Duisburg, Germany

⁶ Bavarian Center for Applied Energy Research (ZAE Bayern), Haberstr. 2a, 91058 Erlangen, Germany

Corresponding Author

*Dr. Derya Baran

Current Address: Center for Plastic Electronics, Department of Chemistry, Imperial College London, London SW7 2AZ, United Kingdom

Telephone number: +44 207594 5866

Current e-mail: d.baran@imperial.ac.uk

1
2
3 **Keywords:** charge transfer states, carrier lifetime, charge collection, organic solar cells, radiative
4
5 open circuit voltage
6
7
8
9

10 11 12 **Abstract**

13
14
15 Non-radiative recombination reduces the open-circuit voltage relative to its theoretical limit and
16
17 leads to reduced luminescence emission at a given excitation. Therefore it is possible to correlate
18
19 changes in luminescence emission with changes in open-circuit voltage and in the charge carrier
20
21 lifetime. Here we use luminescence studies combined with transient photovoltage and
22
23 differential charging analyses to study the effect of polymer fractionation in
24
25 indacenoedithiophene-*co*-benzothiadiazole (IDTBT):fullerene solar cells. In this system,
26
27 polymer fractionation increases electroluminescence emission at the same injection current and
28
29 reduces non-radiative recombination. High molecular weight and fractionated IDTBT polymers
30
31 exhibit higher carrier lifetime-mobility product compared to their non-fractionated analogues,
32
33 resulting in improved solar cell performance.
34
35
36
37
38
39

40 **Introduction**

41
42
43 In polymer:fullerene solar cells, the open-circuit voltage (V_{oc}) is usually limited by
44
45 recombination at the interface between donor and acceptor. Thus, it varies with the energy
46
47 difference between the highest occupied molecular orbital of the donor ($HOMO_D$) and the lowest
48
49 unoccupied molecular orbital of the acceptor ($LUMO_A$).¹⁻³ In practice the $HOMO_D$ - $LUMO_A$
50
51 difference is insufficient to predict V_{oc} due to differences in non-radiative recombination.⁴ The
52
53 highest possible V_{oc} , denoted $V_{oc,rad}$, can be achieved when only radiative recombination occurs
54
55 and the absorbed photon flux is balanced exactly by the emitted flux under open-circuit
56
57
58
59
60

1
2
3 conditions; this is called the radiative limit.⁵⁻¹⁰ In a practical solar cell both V_{oc} and the LED
4 quantum efficiency, Q_{LED} , are reduced relative to their thermodynamic limits by non-radiative
5 recombination pathways, the degree of which can be quantified via a reciprocity theorem.¹¹⁻¹⁷
6
7 Therefore, it is of high interest in the field of organic photovoltaics to reduce these non-radiative
8 recombination losses, thereby bringing the V_{oc} closer to the radiative limit. Recently,
9
10 indacenodithiophene (IDT) copolymers have shown promising field-effect transistor mobilities
11 and solar cell performance.¹⁸⁻²² Enhanced co-planarity of the polymer backbone has been
12 hypothesized to lead to reduced energetic disorder.^{23,24} IDT-*co*-benzothiadiazole polymers have
13 achieved up to 6.5% PCE with device optimization and material purification.²⁵ The role of
14 polymer molecular weight on solar cell performance has been well studied²⁵⁻²⁹; however, the
15 detailed analysis of the recombination processes in fractionated polymer devices remains
16 comparatively unexplored.^{29,30}
17
18
19
20
21
22
23
24
25
26
27
28
29
30
31

32 In this work, we describe how fractionation has an impact on energetic losses and charge
33 transport in IDTBT: PC₇₀BM bulk-heterojunction (BHJ) solar cells. In particular, we use the
34 reciprocity relation between non-radiative recombination and electroluminescence to explain the
35 reduced energetic losses in IDTBT-HM_w: PC₇₀BM solar cells induced by fractionation and
36 higher molecular weight by combining electroluminescence spectroscopy (EL) and Fourier-
37 transform photocurrent spectroscopy (FTPS). The degree of non-radiative recombination,
38 defined as the difference between $V_{oc,rad}$ and V_{oc} and denoted ΔV_{oc} , is found to reduce upon
39 fractionation and with increasing molecular weight. Furthermore, for the same system, we
40 analyze the origin of enhanced photocurrent in terms of charge carrier lifetime and mobility
41 using transient photovoltage (TPV), differential charging, charge extraction (CE) at short circuit
42 and photo-induced charge carrier extraction by linearly increasing voltage technique (photo-
43
44
45
46
47
48
49
50
51
52
53
54
55
56
57
58
59
60

CELIV) measurements. The combination of mobility and lifetime measurements shows that the mobility-lifetime product, which determines charge-carrier collection, is enhanced for the case of high molecular weight devices relative to devices made with low molecular weight and non-fractionated polymers.

Results and Discussion

We studied films and devices made from three IDTBT polymers; IDTBT-NF is not fractionated, and IDTBT-LM_w and IDTBT-HM_w are the low and high molecular weight fractions. The gel permeation chromatography traces and molecular weight information are presented in Figure S1 and Table S1, respectively.

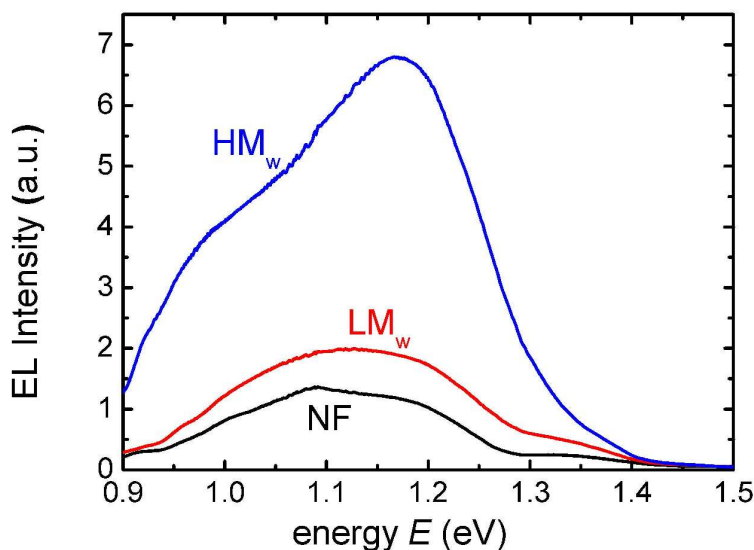


Figure 1 Electroluminescence spectra of IDTBT: PC₇₀BM blend devices at the same current injection of 100 mA cm⁻².

Figure 1 shows the electroluminescence (EL) of IDTBT:PC₇₀BM blend devices, with active layer thicknesses of 75 ±5 nm, was measured under a constant current injection density of 100 mA cm⁻²; the spectral shape of some samples was checked for a range of injection currents down to 22 mA cm⁻² and was found to be independent of current.³¹ The EL intensity increased from the IDTBT-NF: PC₇₀BM blend to the IDTBT-HM_w: PC₇₀BM blend at the same current injection indicating a relatively higher emissive quantum yield for the charge transfer (CT) state for IDTBT-HM_w:PC₇₀BM devices. It can be shown (see the Supporting Information for details) that the voltage loss ΔV_{oc} due to non-radiative recombination can be related to the LED quantum efficiency Q_{LED} via

$$\Delta V_{oc} = V_{oc,rad} - V_{oc} = -\frac{kT}{q} \ln[Q_{LED}]. \quad (1)$$

Here, $V_{oc,rad} \approx kT/q \ln(J_{sc}/J_{0,rad})$ is the radiative limit to the open-circuit voltage, J_{sc} is the device short circuit current density, $J_{0,rad}$ is the saturation current density for radiative recombination and T is the temperature (300 K). The radiative saturation current density ($J_{0,rad}$), is defined as the current due to blackbody radiation (ϕ_{bb}), and can therefore be calculated according to:

$$J_{0,rad} = q \cdot \int_0^{\infty} EQE_{PV}(E) \cdot \phi_{bb}(E) dE \quad (2)$$

where EQE_{PV} is the photovoltaic external quantum efficiency. Similarly, J_{sc} is defined in terms of the solar flux density (ϕ_{sun}):

$$I_{sc} = q \cdot \int_0^{\infty} EQE_{PV}(E) \cdot \phi_{sun}(E) dE \quad (3)$$

At the radiative limit, all the charges recombine radiatively, so the current at short-circuit must be balanced by the radiative current at open-circuit.

We investigated EQE_{PV} , the spectral photovoltaic external quantum efficiency, using FTPS measurements on the same devices in order to determine $V_{oc,rad}$ and hence ΔV_{oc} through the reciprocity relations outlined in the Supporting Information. Figure 2 depicts the experimental EQE_{PV} (solid lines) for blend devices made from IDTBT-NF (Figure 2a), IDTBT-LM_w (Figure 2b) and IDTBT-HM_w (Figure 2c) with PC₇₀BM. For comparison, ϕ_{EL}/ϕ_{bb} , the ratio of the emitted photon flux ϕ_{EL} obtained from electroluminescence for each device to the photon flux ϕ_{bb} expected for a room-temperature black body at the same photon energy, which by reciprocity is another measure of EQE , is also plotted (dashed lines). In all cases polymer absorption is visible at high energies followed by the distinct absorption shoulder of the PC₇₀BM at around 1.8 eV. Below the fullerene absorption shoulder, there is a low energy absorption in the spectrum likely representing the CT state absorption at around 1.40-1.45 eV for IDTBT: PC₇₀BM blends. EQE_{PV} at lower photon energies is estimated from ϕ_{EL}/ϕ_{bb} , which follows experimental EQE_{PV} faithfully at higher energies, as expected from reciprocity.

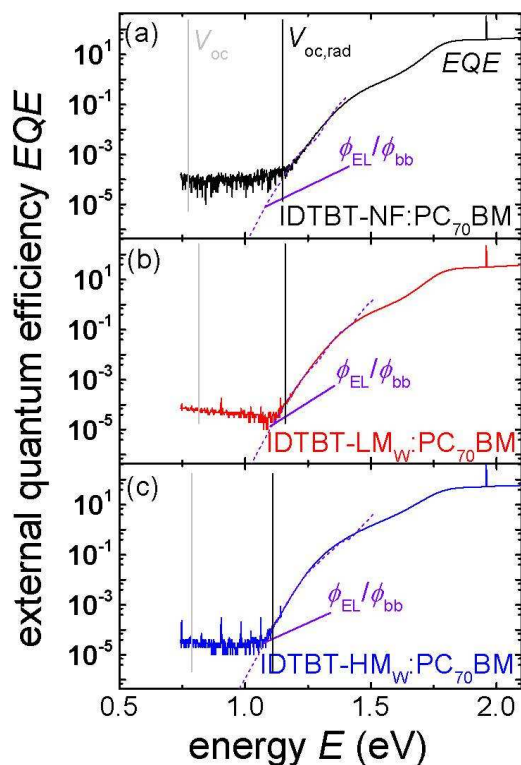


Figure 2 Semi-logarithmic plots of experimental photocurrent external quantum efficiency (EQE_{PV} , solid lines) and calculated EQE_{PV} from EL (dashed lines) as a function of energy for IDTBT-NF/LM_w/HM_w: PC₇₀BM blends (a,b and c respectively).

Table 1 summarizes the values measured and calculated from FTPS and EL measurements. Interestingly, the IDTBT-HM_w device showed the lowest $V_{oc,rad}$ value of 1.11 V, with values of 1.15 and 1.16 V determined for -NF and -LM_w devices respectively. It should be noted that the radiative open-circuit voltage depends on the energetic dependence of EQE_{PV} and so the value of $V_{oc,rad}$ on its own does not indicate merit, but rather the difference between this value and the experimental V_{oc} is pertinent. This ΔV_{oc} , defined by Eq. (1) using Eq. (2) and (3), is found to be 0.37, 0.35 and 0.32 V, for IDTBT-NF, -LM_w and -HM_w, respectively. As seen from Table 1, the IDTBT-HM_w: PC₇₀BM blend yields the lowest radiative open-circuit voltage and the smallest

1
2
3 ΔV_{oc} compared to -LM_w and -NF blends. In addition, the non-fractionated IDTBT-NF: PC₇₀BM
4
5 system has the smallest measured V_{oc} and highest ΔV_{oc} indicating enhanced non-radiative
6
7 recombination in the system. Note that according to Eq. (1), the EL quantum efficiency, obtained
8
9 by integrating the EL spectrum, can also directly yield ΔV_{oc} : the system with the highest Q_{LED}
10
11 value should correspond to the lowest ΔV_{oc} , since non-radiative recombination results in values
12
13 of Q_{LED} less than 1. For polymer:fullerene solar cells the EL is dominated by CT emission with
14
15 typical $Q_{LED} < 10^{-6}$, resulting in a loss in V_{oc} due to non-radiative recombination of over 0.36 V
16
17 at room temperature.³² In this experiment only relative EL flux densities were measured, so the
18
19 differences in ΔV_{oc} between sets of two systems were calculated by dividing the two Q_{LED} values
20
21
22
23
24
25 at the same current injection, i.e.

$$\Delta V_{oc2} - \Delta V_{oc1} = -kT \ln \left[\frac{Q_{LED2}}{Q_{LED1}} \right] \quad (2)$$

26
27
28
29
30
31
32
33 These values were found to agree well with the values calculated using FTPS and EL together
34
35 (see Table S2).
36

37
38
39 The measurement of voltage losses indicates a decrease in non-radiative recombination upon
40
41 increasing the molecular weight of the polymer, so we would expect this effect to be mirrored in
42
43 the recombination lifetime. In disordered photovoltaic materials, charge recombination lifetime,
44
45 like mobility, is charge carrier density dependent and therefore lifetimes must be probed as a
46
47 function of charge density in order to compare different material systems. Therefore transient
48
49 photovoltage (TPV) measurements in combination with differential charging were undertaken;
50
51
52
53 the methods are described in detail elsewhere.³³⁻³⁷
54
55
56
57
58
59
60

Figure 3a displays the charge carrier lifetime from TPV as a function of the charge density obtained from differential charging, showing that carriers in the IDTBT-HM_w devices were much longer lived than carriers in the IDTBT-LM_w and IDTBT-NF devices at the same charge density (corresponding plot of the bimolecular recombination coefficient is shown in Figure S3). It should be noted that the devices measured were all made in the same device run, so any potential differences in the contacts, for example, are minimized; they were however different from the ones used for the EL/FTPS experiment, but showed similar characteristics (Table S4). Therefore, the finding of reduced ΔV_{oc} for IDTBT-HM_w can be assigned to reduced nongeminate recombination, as evidenced by the increase in charge-carrier lifetime. The external LED quantum efficiencies estimated from the values of ΔV_{oc} ($Q_{LED} \approx \exp(-q\Delta V_{oc}/kT)$)¹⁶ are in the range of 10^{-6} to 10^{-7} (Table 1). Thus, changes in radiative recombination have no effect on the total recombination rate and therefore on the charge carrier lifetime.

Table 1 Parameters used in calculation of non-radiative voltage losses^a

Polymers with PC ₇₀ BM	IDTBT-NF	IDTBT-LM _w	IDTBT-HM _w
E_g (eV) ^a	1.7	1.7	1.7
J_{sc} (mA/cm ²) measured ^b	6.9	7.2	10.2
$J_{0,rad}$ (A/cm ²) calc. ^c	3.24×10^{-20}	2.02×10^{-20}	1.63×10^{-19}
$V_{oc,rad}$ (V) calc. ^c	1.150	1.160	1.110
V_{oc} (V) measured ^b	0.775	0.815	0.788
ΔV_{oc} (V) ^d	0.37	0.35	0.32
Q_{LED} at 100 mAcm ⁻²	5.91×10^{-7}	1.28×10^{-6}	4.10×10^{-6}

^a The polymer band gap energy E_g was extrapolated from optical absorption, and is included to emphasize that differences in voltage are not due to the polymer energetics. ^b J_{sc} and V_{oc} were

1
2
3 taken from the J - V curve. ^c $J_{0,\text{rad}}$ and $V_{\text{oc,rad}}$ were calculated from EL and FTPS measurements and
4
5
6 ^d ΔV_{oc} from $V_{\text{oc,rad}} - V_{\text{oc}}$.
7
8

9 In order to evaluate the effect of charge carrier dynamics on solar cell performance, we compare
10 the mobility-lifetime product ($\mu\tau$), a measure of charge carrier collection efficiency, for different
11 systems under similar conditions.^{38,39} Probing the mobility μ with charge extraction at short
12 circuit,⁴⁰ we find only small differences in mobility for the different systems. Since the charge
13 carrier lifetime τ was measured at open circuit and the carrier mobility was measured at short
14 circuit, there is minimal overlap in charge densities between the two measurements. Mobility is
15 not as strongly dependent on charge density as lifetime, so the mobility data were extrapolated
16 over the charge density range of the TPV experiment, thus enabling a calculation of $\mu\tau$. Figure 3b
17 clearly shows that HM_w devices exhibit significantly improved charge carrier collection relative
18 to the NF and LM_w devices, in spite of slightly lower mobility. As a further probe of charge
19 carrier dynamics we measured lifetime and mobility for a similar set of devices using photo-
20 CELIV.^{41,42} Also by this method a significantly higher $\mu\tau$ was observed for the highest molecular
21 weight polymer (Table S5).
22
23
24
25
26
27
28
29
30
31
32
33
34
35
36
37
38
39
40
41
42
43
44
45
46
47
48
49
50
51
52
53
54
55
56
57
58
59
60

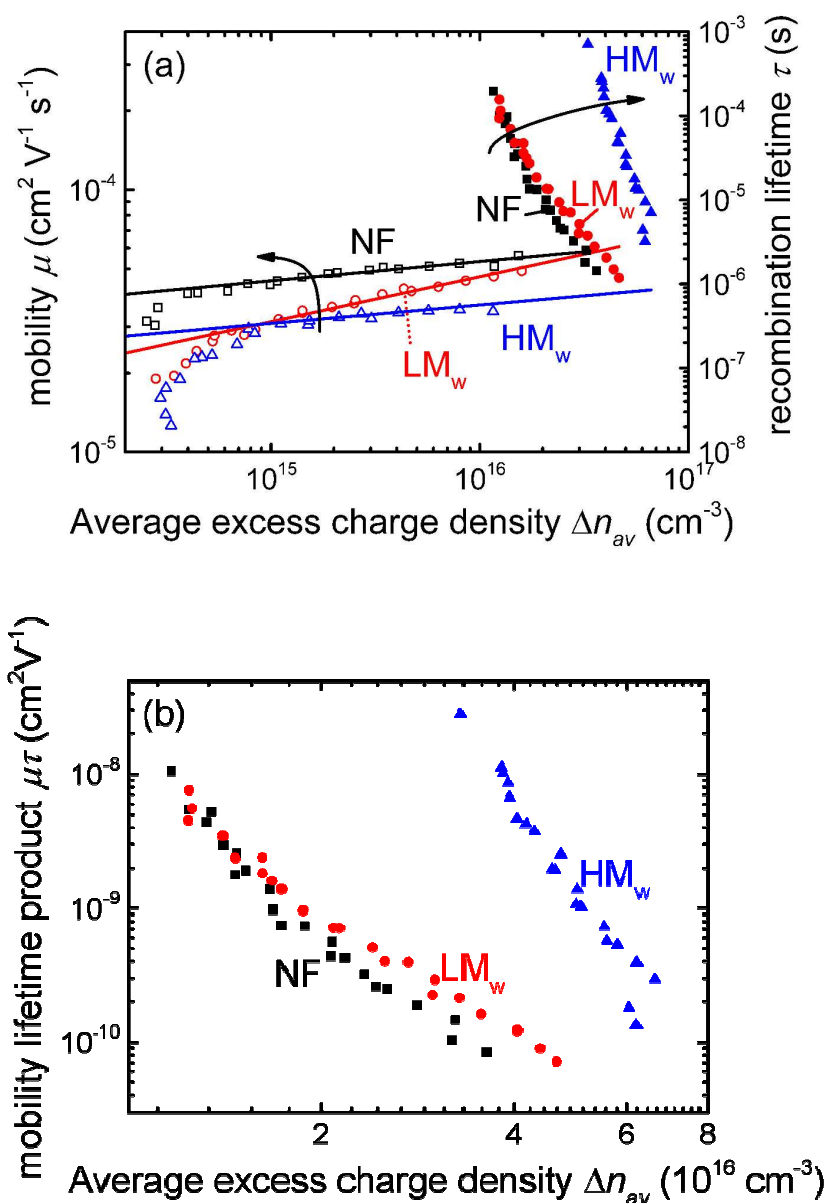


Figure 3 (a) Average carrier mobility, measured by charge extraction at short circuit (open symbols), and recombination lifetime, measured by transient photovoltage (solid symbols). The solid lines are the fits and resulting extrapolation of the mobility data over the charge density range of the transient photovoltage experiment. (b) Mobility-lifetime product, calculated over the charge density range of the lifetime data by extrapolating the mobility data.

1
2
3 The combined measurements of the degree of non-radiative recombination, charge carrier
4 recombination lifetime and mobility for the three sets of devices provide a detailed explanation
5 of the differences we observe in the current-voltage characteristics of solar cells made from these
6 blends (Figure 4). Notably, the J_{sc} of the IDTBT- HM_w : $PC_{70}BM$ devices is significantly greater
7 than that of the $-NF$ and $-LM_w$ devices. This photocurrent enhancement cannot be explained by
8 the polymer optical properties: the absorption and photoluminescence (PL) spectra of the
9 polymers are essentially identical (see Figure S2), as are the device film thicknesses (± 5 nm).
10 Furthermore, addition of $PC_{70}BM$ results in strong PL quenching in the visible region for all
11 polymers, accompanied by intensified emission around 900 nm due to CT state emission. That
12 said, the HM_w blend quenches approximately 50% more than the LM_w and NF blends, which is
13 attributed to more efficient photo-induced charge separation between electron-donating and
14 electron-accepting molecules.⁴²⁻⁴⁵ Moreover, Mott-Schottky analysis of blend devices indicates
15 no difference in the apparent doping concentration before and after fractionation (Figure S6).
16 Therefore it appears that the short-circuit current increase in the HM_w blend is due to a higher
17 efficiency of charge generation and/or charge collection, rather than any kind of optical effect. In
18 addition, there are small differences in the V_{oc} between the devices, which is unexpected since
19 the polymer itself does not change, and the device architectures are identical; however, these
20 differences are explained through differences in the radiative and non-radiative recombination.
21
22
23
24
25
26
27
28
29
30
31
32
33
34
35
36
37
38
39
40
41
42
43
44
45
46
47
48
49
50
51
52
53
54
55
56
57
58
59
60

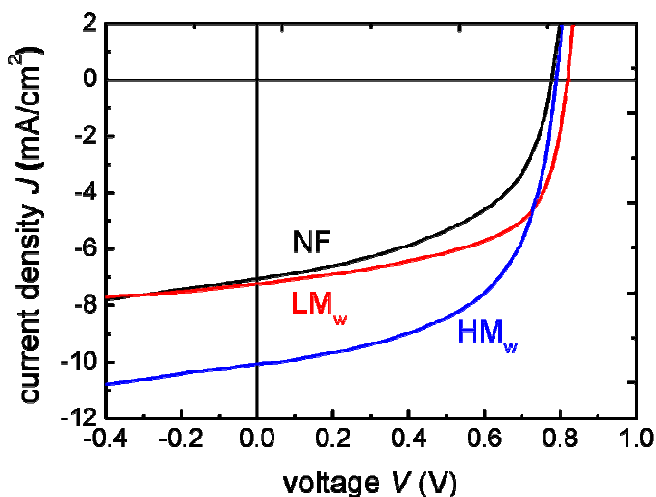


Figure 4 Current-voltage characteristics of the IDTBT-NF, -LM_w and HM_w devices used in this study to measure non-radiative voltage losses (black, red and blue lines respectively). All devices have an ITO / PEDOT:PSS / IDTBT:PC₇₀BM / Ca / Ag architecture.

Conclusion

In summary, we have successfully demonstrated that non-radiative losses can be reduced with fractionation and higher molecular weight in indacenodithiophene copolymers. Analysis of charge dynamics in the bulk-heterojunction devices revealed that increasing the molecular weight of IDTBT polymers increases the carrier lifetime, as anticipated due to the reduced non-radiative voltage losses. The increased lifetime results in an increased mobility-lifetime product, and therefore enhanced carrier collection resulting in an increased J_{sc} . Therefore, this work demonstrates a methodical evaluation of the losses due to non-geminate recombination, and

1
2
3 provides a systematic explanation for the enhanced device performance with molecular weight
4
5 observed in this system.
6
7

8 9 **Experimental Details**

10
11 **Polymer materials.** The polymer materials were synthesized according to Ref [25]. A portion of
12 un-fractionated material, IDTBT-NF, was set aside and the rest was fractionated yielding high
13 and low molecular weight fractions. The gel permeation chromatography traces for the materials
14 are shown in Figure S1 and the corresponding molecular weight information is shown in Table
15 S1.
16
17
18
19
20
21
22
23

24
25 **Fabrication of Photovoltaic devices.** All the devices were fabricated using the doctor-blade
26 technique under ambient conditions. The devices for EL/FTPS and photo-CELIV were made at
27 FAU Erlangen while the devices for TPV/CE were made at Imperial College. Pre-structured
28 indium tin oxide (ITO) substrates were ultrasonic cleaned with acetone and isopropyl alcohol for
29 10 minutes each. After drying the substrates were coated with PEDOT:PSS (around 30 nm) and
30 then 70-90 nm thick active layers based on IDTBT:PC₇₀BM (1:3.5 wt fraction in 1,2-
31 dichlorobenzene) were bladed. The total solution concentration used in Erlangen was 28 mg ml⁻¹
32 while the concentration used at Imperial was 18 mg ml⁻¹; blade coating speeds were adjusted to
33 compensate and achieve similar device thicknesses. To complete the fabrication of the devices
34 15 nm of Ca and 100 nm of Ag were thermally evaporated through a mask (device areas were
35 10.4 mm² (Erlangen) and 4.5 mm² (Imperial)) under vacuum (about 1-5x10⁻⁶ mbar). The *J-V*
36 characteristics were measured using a source measurement unit from BoTest. Illumination was
37 provided by a solar simulator (Oriel Sol 1A, from Newport) with AM1.5G spectrum at 100 mW
38 cm⁻².
39
40
41
42
43
44
45
46
47
48
49
50
51
52
53
54
55
56
57
58
59
60

1
2
3 *EL*. EL measurements were performed by using a chopper and applying a constant current
4 (100mA cm⁻²) supplied by an external current/voltage source through the devices which have an
5 active area of 0.104 cm². The emitted light was then collected by a monochromator and detected
6 by liquid-nitrogen-cooled Ge detector. The spectrum was recorded by a standard lock-in
7 technique. The system was wavelength calibrated.
8
9

10
11
12
13
14
15
16 *FTPS*. FTPS-EQE measurements were carried out using a Vertex 70 from Bruker optics,
17 equipped with QTH lamp, quartz beam splitter and external detector option. A low noise current
18 amplifier (DLPCA-200) is used to amplify the photocurrent produced upon illumination of the
19 photovoltaic devices with light modulated by the FTIR. The output voltage of the current
20 amplifier is fed back to the external detector port of the FTIR, in order to be able to use the
21 FTIR's software to collect the photocurrent spectrum.
22
23
24
25
26
27
28
29

30
31 *Transient photovoltage*. The experimental details are as previously published.³³⁻³⁴
32
33
34
35
36

37 **Current Addresses**

38
39 B. Schroeder

40
41 Current address: Stanford University Shriram Center Department of Chemical Engineering

42
43 443 Via Ortega, Stanford, CA 94305-4125, USA
44
45
46
47

48
49 H. Bronstein

50
51 Department of Chemistry, University College London, Gordon Street, London WC1H 0AJ,

52
53 United Kingdom
54
55
56
57
58
59
60

1
2
3 I. McCulloch
4
5

6 Physical Sciences and Engineering Division, King Abdullah University of Science and
7
8 Technology (KAUST), Thuwal, Saudi Arabia, 23955–6900
9
10

11
12
13
14 **Author Contributions**
15

16
17 ‡These authors contributed equally.
18
19

20
21 **Acknowledgment**
22
23

24 D.B. acknowledges the Bavarian Research Foundation (BFS) and Synthetic carbon allotropes
25 project SFB 953 for financial support. M.S.V. is grateful to the EPSRC for a doctoral training
26 award. J.Y. is grateful to Imperial College for a Rector's scholarship. J.N. acknowledges the
27
28 EPSRC for grants EP/K030671/1, EP/K029843/ and the Supersolar Hub EP/J017361/1, and the
29
30 Royal Society for a Wolfson Merit Award. TK acknowledges the DFG for support via the project
31
32 'Radiative Recombination in Organic Solar Cells'.
33
34
35
36
37
38

39 **Supporting Information Available.** Containing additional experimental details and supporting
40
41 figures. This information is available free of charge via the Internet at <http://pubs.acs.org>
42
43
44
45

46
47 **References**
48
49

- 50 (1) Nelson, J.; Kirkpatrick, J.; Ravirajan, P. Factors Limiting the Efficiency of
51 Molecular Photovoltaic Devices. *Phys. Rev. B* **2004**, *69*, 035337-11.
52 (2) Mutolo, K. L.; Mayo, E. I.; Rand, B. P.; Forrest, S. R.; Thompson, M. E.
53 Enhanced Open-Circuit Voltage in Subphthalocyanine/C60 Organic Photovoltaic Cells. *J. Am.*
54 *Chem. Soc.* **2006**, *128*, 8108-8109.
55
56
57
58
59
60

- 1
- 2
- 3
- 4 (3) Sarangerel, K.; Ganzorig, C.; Fujihira, M.; Sakomura, M.; Ueda, K. Influence of
5 the Work Function of Chemically Modified Indium–Tin–Oxide Electrodes on the
6 Open-circuit Voltage of Heterojunction Photovoltaic Cells. *Chem. Lett.* **2008**, *37*, 778-779.
- 7 (4) Vandewal, K.; Widmer, J.; Heumueller, T.; Brabec, C. J.; McGehee, M.; Leo, K.;
8 Riede, M.; Salleo, A. Increased Open-Circuit Voltage of Organic Solar Cells by Reduced Donor-
9 Acceptor Interface Area. *Adv. Mater.* **2014**, *26*, 3839-3843.
- 10 (5) Ross, R. T. Some Thermodynamics of Photochemical Systems. *J. Chem. Phys.*
11 **1967**, *46*, 4590-4593.
- 12 (6) Shockley, W.; Queisser, H. J. Detailed Balance Limit of Efficiency of P-N
13 Junction Solar Cells. *J. Appl. Phys.* **1961**, *32*, 510-519.
- 14 (7) Kirchartz, T.; Rau, U.; Kurth, M.; Mattheis, J.; Werner, J. H. Comparative Study
15 of Electroluminescence from Cu(In,Ga)Se₂ and Si Solar Cells. *Thin Solid Films* **2007**, *515*,
16 6238-6242.
- 17 (8) Tvingstedt, K.; Malinkiewicz, O.; Baumann, A.; Deibel, C.; Snaith, H. J.;
18 Dyakonov, V.; Bolink, H. J. Radiative efficiency of lead iodide based perovskite solar cells. *Sci.*
19 *Rep.* **2014**, *4*, 6071-7.
- 20 (9) Tress, W.; Marinova, N.; Inganäs, O.; Nazeeruddin, M. K.; Zakeeruddin, S. M.;
21 Graetzel, M. Predicting the Open-Circuit Voltage of CH₃NH₃PbI₃ Perovskite Solar Cells Using
22 Electroluminescence and Photovoltaic Quantum Efficiency Spectra: the Role of Radiative and
23 Non-Radiative Recombination. *Adv. Energy Mater.* **2015**, *5*, 1400812-1400816.
- 24 (10) Yamamoto, S.; Orimo, A.; Ohkita, H.; Benten, H.; Ito, S. Molecular
25 Understanding of the Open-Circuit Voltage of Polymer:Fullerene Solar Cells. *Adv. Energy*
26 *Mater.* **2012**, *2*, 229-237.
- 27 (11) Smestad, G.; Ries, H. Luminescence and Current-Voltage Characteristics of Solar
28 Cells and Optoelectronic Devices. *Sol. Energ. Mat. Sol. C.* **1992**, *25*, 51-71.
- 29 (12) Vandewal, K.; Tvingstedt, K.; Gadisa, A.; Inganas, O.; Manca, J. V. On the
30 Origin of the Open-Circuit Voltage of Polymer-Fullerene Solar Cells. *Nat. Mater.* **2009**, *8*, 904-
31 909.
- 32 (13) Rau, U.; Paetzold, U. W.; Kirchartz, T. Thermodynamics of Light Management in
33 Photovoltaic Devices. *Phys. Rev. B* **2014**, *90*, 035211-16.
- 34 (14) Kirchartz, T.; Rau, U. Electroluminescence Analysis of High Efficiency
35 Cu(In,Ga)Se₂ Solar Cells. *J. Appl. Phys.* **2007**, *102*, 104510-8.
- 36 (15) Kirchartz, T.; Helbig, A.; Reetz, W.; Reuter, M.; Werner, J. H.; Rau, U.
37 Reciprocity between Electroluminescence and Quantum Efficiency Used for the Characterization
38 of Silicon Solar Cells. *Prog. Photovoltaics* **2009**, *17*, 394-402.
- 39 (16) Rau, U. Reciprocity Relation between Photovoltaic Quantum Efficiency and
40 Electroluminescent Emission of Solar Cells. *Phys. Rev. B* **2007**, *76*, 085303-8.
- 41 (17) Gruber, M.; Wagner, J.; Klein, K.; Hörmann, U.; Opitz, A.; Stutzmann, M.;
42 Brütting, W. Thermodynamic Efficiency Limit of Molecular Donor-Acceptor Solar Cells and its
43 Application to Diindenoperylene/C60-Based Planar Heterojunction Devices. *Adv. Energy Mater.*
44 **2012**, *2*, 1100-1108.
- 45 (18) Holliday, S.; Donaghey, J. E.; McCulloch, I. Advances in Charge Carrier
46 Mobilities of Semiconducting Polymers Used in Organic Transistors. *Chem. Mater.* **2013**, *26*,
47 647-663.
- 48
- 49
- 50
- 51
- 52
- 53
- 54
- 55
- 56
- 57
- 58
- 59
- 60

(19) Xu, Y.-X.; Chueh, C.-C.; Yip, H.-L.; Chang, C.-Y.; Liang, P.-W.; Intemann, J. J.; Chen, W.-C.; Jen, A. K. Y. Indacenodithieno[3,2-b]Thiophene-Based Broad Bandgap Polymers for High Efficiency Polymer Solar Cells. *Polym. Chem.* **2013**, *4*, 5220-5223.

(20) Bronstein, H.; Leem, D. S.; Hamilton, R.; Woebkenberg, P.; King, S.; Zhang, W.; Ashraf, R. S.; Heeney, M.; Anthopoulos, T. D.; Mello, J. d.; et al. Indacenodithiophene-co-benzothiadiazole Copolymers for High Performance Solar Cells or Transistors via Alkyl Chain Optimization. *Macromolecules* **2011**, *44*, 6649-6652.

(21) Zhang, X.; Bronstein, H.; Kronemeijer, A. J.; Smith, J.; Kim, Y.; Kline, R. J.; Richter, L. J.; Anthopoulos, T. D.; Siringhaus, H.; Song, K.; et al. Molecular Origin of High Field-Effect Mobility in an Indacenodithiophene-Benzothiadiazole Copolymer. *Nat. Commun.* **2013**, *4*, 2238-46.

(22) Venkateshvaran, D.; Nikolka, M.; Sadhanala, A.; Lemaur, V.; Zelazny, M.; Kepa, M.; Hurhangee, M.; Kronemeijer, A. J.; Pecunia, V.; Nasrallah, I. et al. Approaching Disorder-Free Transport in High-Mobility Conjugated Polymers. *Nature* **2014**, *515*, 384-388.

(23) McCulloch, I.; Ashraf, R. S.; Biniek, L.; Bronstein, H.; Combe, C.; Donaghey, J. E.; James, D. I.; Nielsen, C. B.; Schroeder, B. C.; Zhang, W. Design of Semiconducting Indacenodithiophene Polymers for High Performance Transistors and Solar Cells. *Acc. Chem. Res.* **2012**, *45*, 714-722.

(24) Zhang, Y.; Zou, J.; Yip, H.-L.; Chen, K.-S.; Zeigler, D. F.; Sun, Y.; Jen, A. K. Y. Indacenodithiophene and Quinoxaline-Based Conjugated Polymers for Highly Efficient Polymer Solar Cells. *Chem. Mater.* **2011**, *23*, 2289-2291.

(25) Ashraf, R. S.; Schroeder, B. C.; Bronstein, H. A.; Huang, Z.; Thomas, S.; Kline, R. J.; Brabec, C. J.; Rannou, P.; Anthopoulos, T. D.; Durrant, J. R.; et al. The influence of Polymer Purification on Photovoltaic Device Performance of a Series of Indacenodithiophene Donor Polymers. *Adv. Mater.* **2013**, *25*, 2029-2034.

(26) Müller, C.; Wang, E.; Andersson, L. M.; Tvingstedt, K.; Zhou, Y.; Andersson, M. R.; Inganäs, O. Influence of Molecular Weight on the Performance of Organic Solar Cells Based on a Fluorene Derivative. *Adv. Funct. Mater.* **2010**, *20*, 2124-2131.

(27) Ma, W.; Kim, J. Y.; Lee, K.; Heeger, A. J. Effect of the Molecular Weight of Poly(3-hexylthiophene) on the Morphology and Performance of Polymer Bulk Heterojunction Solar Cells. *Macromol. Rapid Commun.* **2007**, *28*, 1776-1780.

(28) Ballantyne, A. M.; Chen, L.; Dane, J.; Hammant, T.; Braun, F. M.; Heeney, M.; Duffy, W.; McCulloch, I.; Bradley, D. D. C.; Nelson, J. The Effect of Poly(3-hexylthiophene) Molecular Weight on Charge Transport and the Performance of Polymer:Fullerene Solar Cells. *Adv. Funct. Mater.* **2008**, *18*, 2373-2380.

(29) Huang, Z.; Fregoso, E. C.; Dimitrov, S.; Tuladhar, P. S.; Soon, Y. W.; Bronstein, H.; Meager, I.; Zhang, W.; McCulloch, I.; Durrant, J. R. Optimisation of Diketopyrrolopyrrole:Fullerene Solar Cell Performance Through Control of Polymer Molecular Weight and Thermal Annealing. *J. Mater. Chem. A* **2014**, *2*, 19282-19289.

(30) Dimitrov, S. D.; Huang, Z.; Deledalle, F.; Nielsen, C. B.; Schroeder, B. C.; Ashraf, R. S.; Shoaee, S.; McCulloch, I.; Durrant, J. R. Towards Optimisation of Photocurrent From Fullerene Excitons in Organic Solar Cells. *Energ. Environ. Sci.* **2014**, *7*, 1037-1043.

(31) Gong, W.; Faist, M. A.; Ekins-Daukes, N. J.; Xu, Z.; Bradley, D. D. C.; Nelson, J. Kirchartz, T. Influence of Energetic Disorder on Electroluminescence Emission in Polymer:Fullerene Solar Cells. *Phys. Rev. B.* **2012**, *86*, 024201-9.

(32) Vandewal, K.; Ma, Z.; Bergqvist, J.; Tang, Z.; Wang, E.; Henriksson, P.; Tvingstedt, K.; Andersson, M. R.; Zhang, F.; Inganäs, O. Quantification of Quantum Efficiency and Energy Losses in Low Bandgap Polymer:Fullerene Solar Cells with High Open-Circuit Voltage. *Adv. Funct. Mater.* **2012**, *22*, 3480-3490.

(33) Shuttle, C. G.; O'Regan, B.; Ballantyne, A. M.; Nelson, J.; Bradley, D. D. C.; de Mello, J.; Durrant, J. R. Experimental Determination of the Rate Law for Charge Carrier Decay in a Polythiophene: Fullerene Solar Cell. *Appl. Phys. Lett.* **2008**, *92*, 093311-3.

(34) Maurano, A.; Shuttle, C. G.; Hamilton, R.; Ballantyne, A. M.; Nelson, J.; Zhang, W.; Heeney, M.; Durrant, J. R. Transient Optoelectronic Analysis of Charge Carrier Losses in a Selenophene/Fullerene Blend Solar Cell. *J. Phys. Chem. C* **2011**, *115*, 5947-5957.

(35) Shuttle, C.; O'Regan, B.; Ballantyne, A.; Nelson, J.; Bradley, D.; Durrant, J. Bimolecular Recombination Losses in Polythiophene: Fullerene Solar Cells. *Phys.Rev. B* **2008**, *78*, 113201-4.

(36) Credgington, D.; Hamilton, R.; Atienzar, P.; Nelson, J.; Durrant, J. R. Non-Geminate Recombination as the Primary Determinant of Open-Circuit Voltage in Polythiophene:Fullerene Blend Solar Cells: an Analysis of the Influence of Device Processing Conditions. *Adv. Funct. Mater.* **2011**, *21*, 2744-2753.

(37) Credgington, D.; Durrant, J. R. Insights from Transient Optoelectronic Analyses on the Open-Circuit Voltage of Organic Solar Cells. *J. Phys. Chem. Lett.* **2012**, *3*, 1465-1478.

(38) Schilinsky, P.; Waldauf, C.; Brabec, C. J. Recombination and loss Analysis in Polythiophene Based Bulk Heterojunction Photodetectors. *Appl. Phys. Lett.* **2002**, *81*, 3885-3887.

(39) Hawks, S. A.; Deledalle, F.; Yao, J.; Rebois, D. G.; Li, G.; Nelson, J.; Yang, Y.; Kirchartz, T.; Durrant, J. R. Relating Recombination, Density of States, and Device Performance in an Efficient Polymer: Fullerene Organic Solar Cell Blend. *Adv. Energy Mater.* **2013**, *3*, 1201-1209.

(40) Shuttle, C. G.; Hamilton, R.; Nelson, J.; O'Regan, B. C.; Durrant, J. R. Measurement of Charge-Density Dependence of Carrier Mobility in an Organic Semiconductor Blend. *Adv. Funct. Mater.* **2010**, *20*, 698-702.

(41) Mozer, A. J.; Sariciftci, N. S.; Lutsen, L.; Vanderzande, D.; Österbacka, R.; Westerling, M.; Juška, G. Charge transport and Recombination in Bulk Heterojunction Solar Cells Studied by the Photoinduced Charge Extraction in Linearly Increasing Voltage Technique. *Appl. Phys. Lett.* **2005**, *86*, 112104-3.

(42) Gasparini, N.; Katsouras, A.; Prodromidis, M. I.; Avgeropoulos, A.; Baran, D.; Salvador, M.; Fladischer, S.; Spiecker, E.; Chochos, C. L.; Ameri, T.; Brabec, C. J. Photophysics of Molecular-Weight-Induced Losses in Indacenodithienothiophene-Based Solar Cells. *Adv. Funct. Mater.* **2015**, DOI: 10.1002/adfm.201501062.

(43) Snaith, H. J.; Arias, A. C.; Morteani, A. C.; Silva, C.; Friend, R. H. Charge Generation Kinetics and Transport Mechanisms in Blended Polyfluorene Photovoltaic Devices. *Nano Lett.* **2002**, *2*, 1353-1357.

(44) Kim, Y.; Cook, S.; Choulis, S. A.; Nelson, J.; Durrant, J. R.; Bradley, D. D. C. Organic Photovoltaic Devices Based on Blends of Regioregular Poly(3-hexylthiophene) and Poly(9,9-dioctylfluorene-co-benzothiadiazole). *Chem. Mater.* **2004**, *16*, 4812-4818.

(45) Baran, D.; Li, N.; Breton, A.-C.; Osvet, A.; Ameri, T.; Leclerc, M.; Brabec, C. J. Qualitative Analysis of Bulk-Heterojunction Solar Cells without Device Fabrication: An Elegant and Contactless Method. *J. Am. Chem. Soc.* **2014**, *136*, 10949-10955.

1	
2	
3	
4	
5	
6	
7	
8	
9	
10	
11	
12	
13	
14	
15	
16	
17	
18	
19	
20	
21	
22	
23	
24	
25	
26	
27	
28	
29	
30	
31	
32	
33	
34	
35	
36	
37	
38	
39	
40	
41	
42	
43	
44	
45	
46	
47	
48	
49	Table of Content Entry (TOC)
50	
51	
52	
53	
54	
55	
56	
57	
58	
59	
60	

